Neuro-Oncology Advances

6(1), vdae059, 2024 | https://doi.org/10.1093/noajnl/vdae059 | Advance Access date 18 April 2024

Chromothripsis is rare in IDH-mutant gliomas compared to IDH-wild-type glioblastomas whereas whole-genome duplication is equally frequent in both tumor types

Baptiste Sourty, Laëtitia Basset, Alix Fontaine, Emmanuel Garcion, and Audrey Rousseau

All author affiliations are listed at the end of the article

Corresponding Author: Audrey Rousseau, MD, PhD, Department of Pathology, Angers University Hospital, 4 rue Larrey, 49933 Angers, France (aurousseau@chu-angers.fr).

Abstract

Background. Adult-type diffuse gliomas comprise *IDH* (*isocitrate dehydrogenase*)-mutant astrocytomas, *IDH*-mutant 1p/19q-codeleted oligodendrogliomas (ODG), and *IDH*-wild-type glioblastomas (GBM). GBM displays genome instability, which may result from 2 genetic events leading to massive chromosome alterations: Chromothripsis (CT) and whole-genome duplication (WGD). These events are scarcely described in *IDH*-mutant gliomas. The better prognosis of the latter may be related to their genome stability compared to GBM.

Methods. Pangenomic profiles of 297 adult diffuse gliomas were analyzed at initial diagnosis using SNP arrays, including 192 GBM and 105 *IDH*-mutant gliomas (61 astrocytomas and 44 ODG). Tumor ploidy was assessed with *Genome Alteration Print* and CT events with *CTLPScanner* and through manual screening. Survival data were compared using the Kaplan–Meier method.

Results. At initial diagnosis, 37 GBM (18.7%) displayed CT versus 5 *IDH*-mutant gliomas (4.7%; $P = .0008$), the latter were all high-grade (grade 3 or 4) astrocytomas. WGD was detected at initial diagnosis in 18 GBM (9.3%) and 9 *IDH*-mutant gliomas (5 astrocytomas and 4 oligodendrogliomas, either low- or high-grade; 8.5%). Neither CT nor WGD was associated with overall survival in GBM or in *IDH*-mutant gliomas.

Conclusions. CT is less frequent in *IDH*-mutant gliomas compared to GBM. The absence of CT in ODG and grade 2 astrocytomas might, in part, explain their genome stability and better prognosis, while CT might underlie aggressive biological behavior in some high-grade astrocytomas. WGD is a rare and early event occurring equally in *IDH*-mutant gliomas and GBM.

Key Points

- Chromothripsis is less frequent in *IDH*-mutant gliomas compared to glioblastomas.
- Chromothripsis may occur in grade 3 or 4 *IDH*-mutant astrocytomas but not in oligodendrogliomas.
- Whole-genome duplication is equally rare in *IDH*-mutant gliomas and glioblastomas.

Adult-type diffuse gliomas are the most frequent primary central nervous system tumors. They are classified based on *IDH1/2* (*isocitrate dehydrogenase 1/2*) gene status according to the 2021 WHO classification: *IDH*-mutant (*IDH*m) astrocytomas, *IDH*m 1p/19q-codeleted oligodendrogliomas (ODG), and *IDH*-wild-type glioblastomas (GBM).[1] Most *IDH*m astrocytomas display *ATRX* and *TP53* mutations (the latter mostly occurring in the context of a copy-neutral loss of heterozygosity (CNLOH) of chromosome (chr) 17p), whereas all ODG are characterized by the combined loss of chr arms 1p and 19q (1p/19q codeletion).[1] *IDH1/2* mutation and 1p/19q codeletion are independently associated with a better prognosis, hence

Importance of the Study

The present study focused on the detection of 2 genetic events linked to genome instability in adult-type diffuse gliomas. Chromothripsis (CT) has been seldom described in *IDH*-mutant gliomas and whole-genome duplication (WGD) has never been investigated. We compared their occurrence in *IDH*-mutant gliomas versus *IDH*-wild-type glioblastomas (GBM). CT was significantly less frequent in *IDH*-mutant gliomas as a whole compared to GBM, reflecting the former's greater genome stability. The absence of CT in oligodendrogliomas and grade 2 astrocytomas might, in part, explain their better prognosis, while CT might contribute to more aggressive biological behavior in higher-grade astrocytomas. We investigated for the first time WGD in *IDH*-mutant gliomas: This early event was as rare as in GBM, preceding most chromosome losses and promoting aneuploidy. This work highlights key genomic features of *IDH*-mutant gliomas compared to GBM. Detecting CT events in *IDH*-mutant gliomas might help anticipate disease progression and adapt treatments.

the longer overall survival (OS) in ODG compared to astrocytomas.[1–3] By contrast, GBM are aggressive WHO grade 4 tumors whose median OS is 15 to 18 months after standard of care treatment.[4] GBM are characterized by numerous copy-number variations (CNV), which are a hallmark of genome instability.[1] The latter is defined by the accumulation of chr gains and/or losses (ie, copy-number alterations and resulting in aneuploidy) and chr rearrangements (ie, structural alterations).[5] Such chromosome instability (CIN) has been associated with rapid-onset genetic events leading to massive genome rearrangement (known as "macro-evolutive" events) and accelerating tumorigenesis or tumor progression.[6]

Among such events, whole-genome duplication (WGD) results in genome doubling (tetraploidy instead of diploidy). WGD is the second most common genetic event in tumorigenesis (after *TP53* inactivation), occurring in about 30% of carcinomas.[7] WGD has been reported in 11% of GBM in 2 independent studies.[8,9] By increasing gene dosage, WGD may allow tumors to survive potentially deleterious somatic mutations.[7,10] It has been found to confer a selective advantage in many cancer types, leading to an adverse prognosis.[7,11,12]

Chromothripsis (CT) was first described in 2011 by Stephens et al. as a cataclysmic event consisting in the shattering of one (or a few) chr in tens to hundreds of pieces that are haphazardly reassembled in a derivative chr.[13] CT causes many chr losses leading to tumor suppressor gene inactivation, chr inversions or translocations (contributing to gene fusions), and oncogene amplifications (often as double-minute chr).[9,14–18] Thus, CT results in a massive, spatially confined, genome remodeling. CT is more frequent than originally thought, detected in about 30% of cancers and > 50% of GBM using high-throughput sequencing.[19] In the central nervous system, CT has been described in medulloblastomas and supra-tentorial ependymomas (involving the *ZFTA* locus on chr 11).[20,21] CT underlies driver events in GBM, such as *EGFR*, *MDM2*, and *CDK4* gene amplifications.[9,22]

Chaos-driving genomic events such as WGD and CT remain scarcely described in *IDH*m gliomas, whereas they have been reported in GBM. We hypothesized that the better prognosis of *IDH*m gliomas compared to GBM might be related, at least in part, to the rarity of WGD and CT resulting in a higher genome stability.

Material and Methods

Cohort

This retrospective cohort comprised 297 adult-type diffuse gliomas (61 *IDH*m astrocytomas, 44 *IDH*m 1p/19q-codeleted ODG, and 192 *IDH*-wild-type GBM). All patients were >18 years old and were operated on at Angers University Hospital, between 2012 and 2022 for the *IDH*m gliomas and between 2017 and 2021 for the GBM. Only cases for which Single Nucleotide Polymorphism (SNP) arrays had previously been performed on fresh-frozen material were included in the study. Fresh-frozen tumor samples were obtained from the biobank of Angers University Hospital, after written informed consent was obtained from patients, in agreement with the requirements of our institutional review board (DC-2011-1467/ AC-2017-2993). Clinical, histopathological, and molecular data were available for all patients. The database was registered with the French Data Protection Authority (CNIL, n°ar22-0009v0). All cases had been diagnosed by 2 neuropathologists and were reclassified according to the 2021 WHO classification.[1]

IDH1/2 Status

Immunostaining for IDH1-R132H mutant protein (clone H09; Dianova, Switzerland) was performed on 4 µm-thick formalin-fixed paraffin-embedded tissue sections in the automated *BOND-III* (Leica Biosystems, Germany). For patients < 55 years old, Sanger sequencing was performed to detect rare *IDH1/2* mutations, as described elsewhere.[9]

SNP Arrays

SNP arrays were performed on the 297 cases. Tumor DNA was extracted from fresh-frozen tissue using the *NucleoSpin Tissue kit* (Macherey-Nagel, France) according to the manufacturer's instructions and quantified using the *Qubit dsDNA BR Assay Kit* (Life Technologies, USA). Tumor DNA was amplified, fragmented using *Infinium homozygous deletion (HD) Assay Ultra Protocol* (Illumina, USA), and hybridized using *Infinium CytoSNP-850K Illumina Beadchips* (Illumina, USA) according to the manufacturer's

instructions. DNA bead chips were scanned on the *iScan* system (Illumina, USA). Data were analyzed using the software *GenomeStudio v2011.1* (Illumina, USA).

Ploidy and Copy-Number Analyses

The bioinformatic method *Genome Alteration Print* was used to determine the chr number and ploidy (namely 2n [diploidy] or 4n [tetraploidy]) for each tumor, and to detect segmental copy number and allelotype (heterozygote or homozygote) of complex genomic profiles obtained through SNP arrays.[23] The SNP array data were deposited in the public repository ArrayExpress under the accession number E-MTAB-13542. The occurrence of the chr losses in relation to WGD (before or after WGD) was estimated based on the allelotype of the chr segments involved. Retention of heterozygosity of a given segment displaying copy-number loss in a tetraploid tumor (ie, copy number < 4) implies that WGD occurred before the chr loss, whereas chr losses occurring prior to WGD lead to a definitive loss of heterozygosity, that cannot be overturned through duplication of the remaining allele during WGD.

CT Screening and Validation

CT was detected using segmented data from *GenomeStudio* SNP arrays in a two-step procedure. First, visual screening was performed by the same observer following predefined and previously published criteria, including: (1) clustering of chr breakpoints on one (or rarely 2) chr arm(s), (2) regularity of oscillating copy-number states (mostly 2 or 3 copy-number states), and (3) interspersed loss and retention of heterozygosity.[24] Second, a validation analysis was carried out for all cases using the algorithm-based server *CTLPScanner*, allowing to detect of CT patterns, with the following scanner parameters and thresholds: genome assembly = GRCh37/hg19; copy-number status change times ≥ 10; log10 of likelihood ratio ≥ 8, minimum segment size (Kb): 10; signal distance between adjacent segments: 0.3; signal value for genomic gains/losses ≥ or ≤ 0.15.[25] The results obtained with both methods were compared: Only cases validated by *CTLPScanner* were retained as positive for CT; on the other hand, all cases positive for CT according to *CTLPScanner* that had not been visually detected were reviewed by 2 observers to confirm or dismiss the presence of CT.

Survival Data

OS data were obtained from the electronic files of the patients at Angers University Hospital and from the open-access INSEE database (https://deces.matchid.io/search).

Statistical Analyses

Categorical variables were expressed as absolute values and percentages; continuous variables as median and mean values. Chi-square test or Fisher's exact test was used to compare the distribution of categorical variables and Wilcoxon-Mann–Whitney test to compare the distribution of continuous variables. OS was defined as the time from histopathological diagnosis to death or last follow-up, with patients still alive at last follow-up reported as a censored event. OS rates were compared according to the Kaplan–Meier method with the log-rank test. Statistical analyses were performed using *Excel* software (version 2010, Microsoft), open-access website *BiostaTGV* (https://biostatgv.sentiweb.fr/), and *GraphPad Prism* (version 9). *P*-value < .05 was considered statistically significant.

Results

Clinical and Histopathological Characteristics

At initial diagnosis, 105 *IDH*m gliomas and 192 GBM were included in the study. *IDH*m gliomas comprised 61 astrocytomas (7 grade 2, 42 grade 3, and 12 grade 4) and 44 ODG (16 grade 2 and 28 grade 3). Among them, 16 cases (16/105, 15.2%) were analyzed both at initial diagnosis and at recurrence. These paired samples comprised 11 astrocytomas (1 grade 2, 3 grade 3, and 7 grade 4) and 5 ODG (2 grade 2 and 3 grade 3). In addition to the 105 *IDH*m gliomas, 24 *IDH*m gliomas whose pangenomic SNP array profile at initial diagnosis was not available were analyzed at recurrence only, in order to investigate the presence of CT and/or WGD. This group comprised 15 astrocytomas (7 grade 3 and 8 grade 4) and 9 ODG (all grade 3). The characteristics of the cohort are detailed in Supplementary Table S1.

Among the 105 *IDH*m gliomas at initial diagnosis, 89 cases were immunopositive for IDH1-R132H mutant protein (84.7%). Among the 24 *IDH*m gliomas analyzed only at recurrence, 18 cases were immunopositive for IDH1-R132H mutant protein (75%). The remaining cases of initial and recurrent gliomas displayed *IDH1/2* mutation via sequencing.

The median age at diagnosis was 43 years old for *IDH*m gliomas and 63 years old for GBM. Among the *IDH*m gliomas, median age at diagnosis was 46.5 years old for ODG (grade 2: 38 years old, grade 3: 51.5 years old) and 42 years old for astrocytomas (grade 2 and grade 3: 41 years old, grade 4: 49 years old). The male/female ratio was 1.4 for *IDH*m gliomas (1.2 for ODG and 1.7 for astrocytomas) and 1.3 for GBM. Median OS was 13 months for GBM. It was 135 months and 63 months for grades 3 and 4 *IDH*m astrocytomas, respectively. It was 261 months for grade 3 ODG. Median OS was not reached for grade 2 *IDH*m gliomas.

Copy-Number Alterations

Pangenomic profiles of diploid tumors (ie, without WGD) at chr arm-level are presented in Figure 1 for *IDH*m gliomas at initial diagnosis and in Figure 2 for GBM. Pangenomic profiles of tetraploid tumors (ie, with WGD) at chr arm-level in *IDH*m gliomas at initial diagnosis and in GBM are presented in Figure 3. With regard to relevant focal (gene-level) CNV in diploid *IDH*m gliomas, *CDKN2A/B* HD was detected at initial diagnosis in 3 astrocytomas (grade 4) and one ODG (grade 3), and at recurrence in 6 astrocytomas (5 of them without initial tumor available) and one ODG

Figure 1. Arm-level CNV landscape of the 96 diploid *IDH*-mutant gliomas (without WGD) at initial diagnosis. All ODG displayed 1p/19q codeletion with few additional CNV compared to astrocytomas. CNV burden was higher in grade 3 versus 2 ODG but the genome remained overall relatively stable. The most common CNV in astrocytomas was CNLOH of chr 17p (46/61, 75%). CNV burden increased in astrocytomas from grade 2 through 4. The cases displayed recurrent chr 7q gain. Three astrocytomas harbored CT at initial diagnosis. "Complex chromosome rearrangement" encompasses all genomic profiles with numerous CNV which cannot be precisely classified, some of them displaying CT patterns. "Partial chromosome gain and loss" indicates the presence of segments with copy-number gains and losses extending > one chromosome band. Chr, chromosome; CNLOH, copy-neutral loss of heterozygosity; CNV, copy-number variation; CT, chromothripsis; ODG, oligodendroglioma; WGD, whole-genome duplication.

(grade 3; no initial tumor available). In diploid GBM, *CDKN2A/B* HD was detected in 103/174 cases (59.1%) and *PTEN* HD in 18/174 cases (10.3%). *CDKN2A/B* and *PTEN* HD were assessed in diploid tumors, since chr losses in tetraploid tumors, which harbor supernumerary copies, give rise to intermediate copy-number levels. In all GBM (diploid or tetraploid), *EGFR* amplification was detected in 73/192 cases (38%), *CDK4* amplification in 31/192 cases (16.1%), *MDM2* and *MDM4* amplification in 14/192 cases each (7.2%), *PDGFRA* amplification in 9/192 cases (4.6%), and *MET* amplification in 5/192 cases (2.6%). *CDK4* and *MDM2* were co-amplified in 9/192 cases (4.6%). We detected *MYCN* amplification in one GBM case. A detailed list of the gene alterations is presented in Supplementary

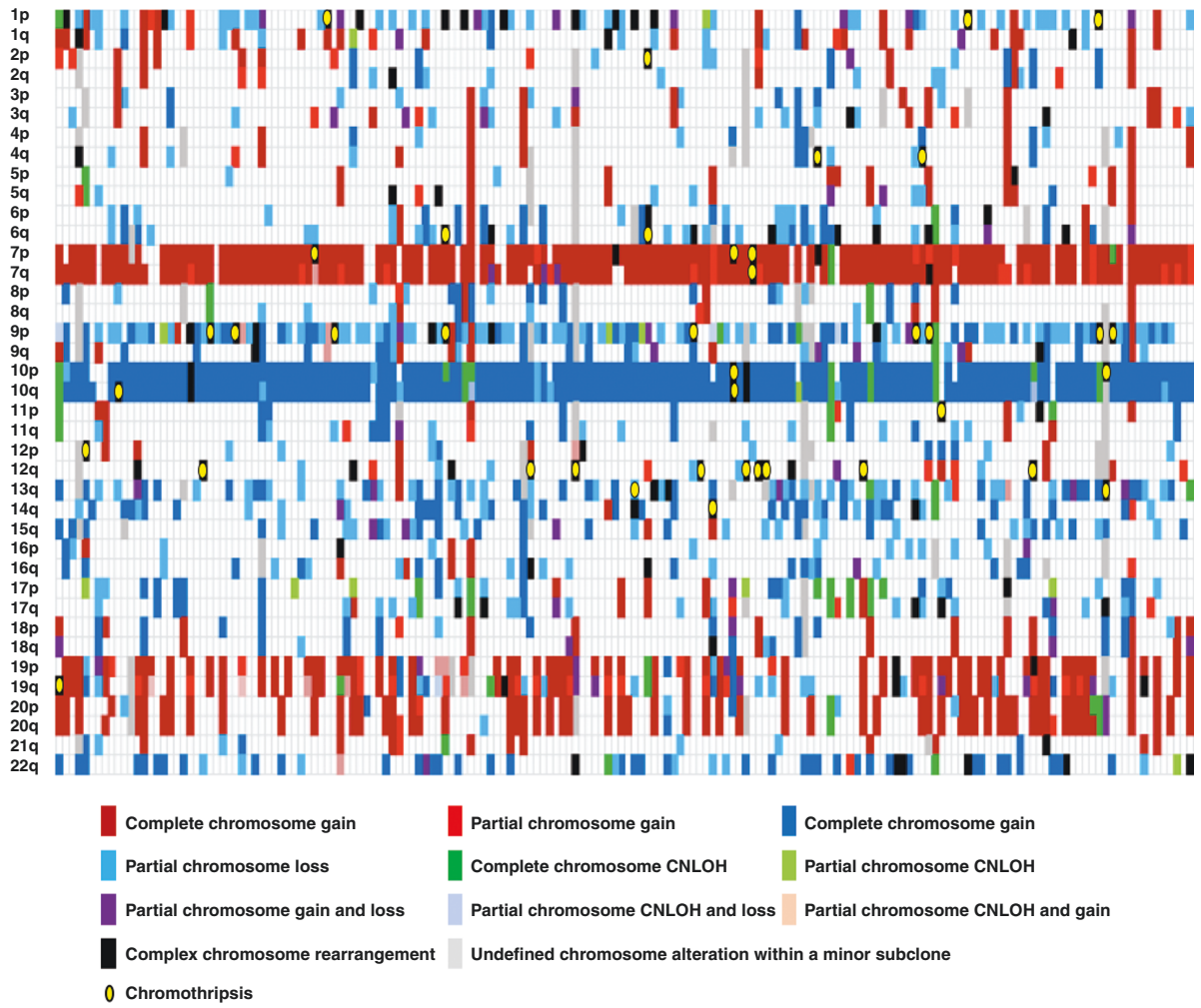

Figure 2. Arm-level CNV landscape of the 174 diploid GBM (without WGD) at initial diagnosis. The most common CNV were chr 7 gain, chr 9p loss, chr 10 loss, chr 19 gain, and chr 20 gain. Chr 10 loss was detected in 170/174 GBM (97.7%) and chr 7 gain in 156/174 GBM (89.6%). Thirty-three GBM displayed CT, mostly on chr 12q (*MDM2/CK4* loci) and chr 9p (*CDKN2A/B* locus). "Complex chromosome rearrangement," "partial chromosome gain and loss," and abbreviations as in Figure 1.

Table S2. CNV detected in *IDH*m gliomas versus their recurrence (if available) are presented in Supplementary Figure S1. The CNV load in recurrent ODG was overall comparable to that in the corresponding initial tumors (even in grade 3 ODG) whereas in astrocytomas, the CNV load increased with grade and in recurrent versus initial tumors.

WGD is as Frequent in *IDHm* Gliomas as in GBM

In *IDH*m gliomas, WGD was detected in 9 cases at initial diagnosis (9/105, 8.5%), including 5 astrocytomas (5/61, 8.2%; 1 grade 2, 3 grade 3, and 1 grade 4) and 4 ODG (4/44, 9.1%; 1 grade 2, 3 grade 3). In GBM, WGD was detected in 18/192 cases (9.3%). The frequency of WGD did not significantly differ between *IDH*m gliomas and GBM (8.5% versus 9.3%, $P = .8178$, chi-square test). Examples of WGD in *IDH*m gliomas are shown in Figure 4A–B.

In tetraploid *IDH*m gliomas at initial diagnosis, the mean chr number per tumor was 85 (66.5 to 91.5; for a theoretical number of 92 [4n]) for both astrocytomas and ODG. At recurrence, 2 grade 4 astrocytomas harbored WGD (one without WGD at initial diagnosis, the other without initial tumor available), with a chr number of 88.5 and 87, respectively. Diploid *IDH*m gliomas had a mean chr number of 46.4 (42.5 to 52.5; 45.5 for ODG and 47 for astrocytomas; theoretical number of 46 [2n]). Tetraploid GBM displayed a mean chr number of 85 (62.5 to 96.5), while diploid GBM had a mean number of 48.7 (39.5 to 57). Hence, the mean chr number in WGD tumors was lower than expected, both in *IDH*m gliomas and GBM (85 chr each). Inversely, the chr number in tumors without WGD was closer to what was expected.

Overall, within the limits of the small sample size, there was an increased number of total CNV in WGD tumors compared to diploid tumors and in high-grade (grade 3 or 4) versus lower-grade gliomas (Figures 1 and 3). The mean number of CNV-harboring chr arms was higher in GBM with WGD than without (22 vs. 17.5, respectively, $P = .0002$,

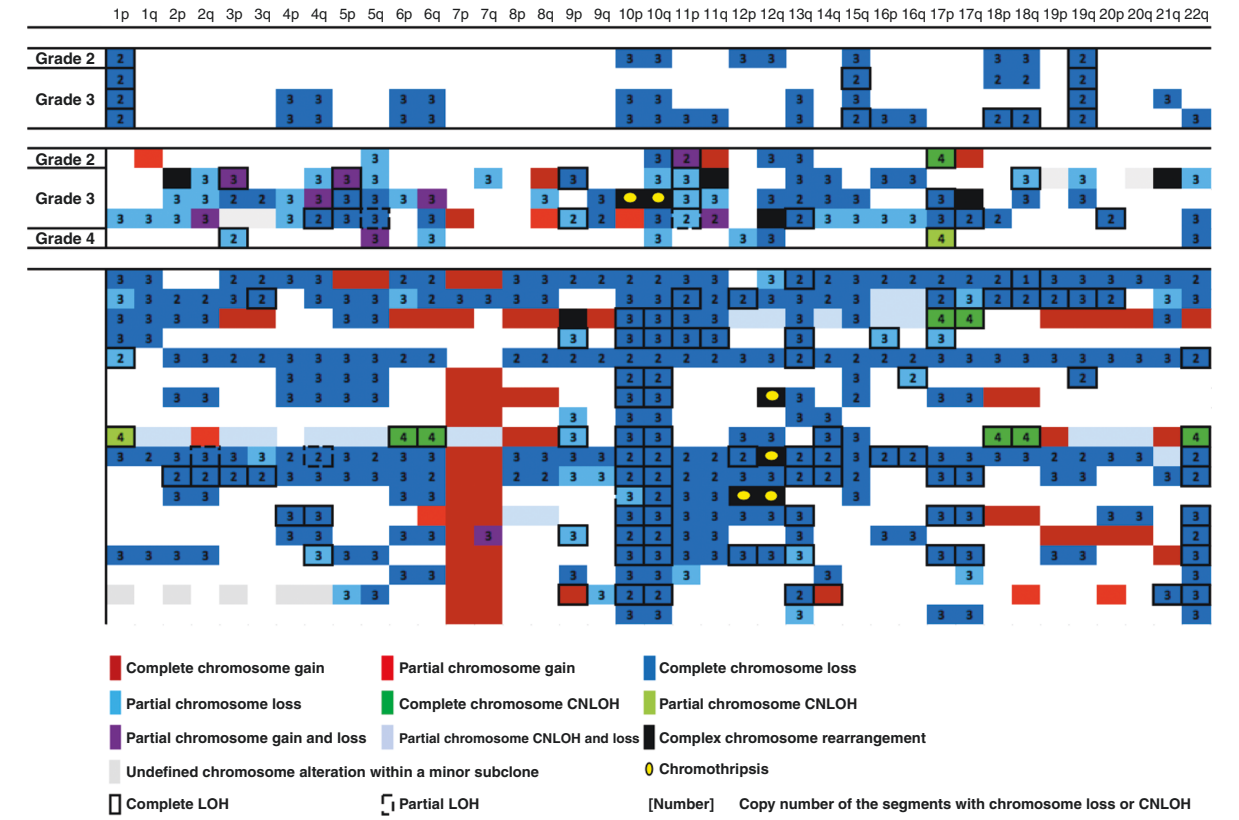

Figure 3. Arm-level CNV landscape of the 9 WGD *IDH*-mutant gliomas and 18 WGD GBM at initial diagnosis. Each line corresponds to a sample. All ODG displayed 1p/19q codeletion with complete LOH. Most astrocytomas (4/5 cases) displayed 17p loss or CNLOH. All GBM harbored chr 10 loss (mainly with complete LOH), while most of them (14/18) harbored partial or whole chr 7 gain. CT was detected in one astrocytoma (on chr 10) and 3 GBM (2 on chr 12q and 1 on the whole chr 12). Most tumors displayed numerous whole chr arm-level losses (shedding of excess DNA). Black squares indicate if the chr losses are associated with LOH (complete or partial), as heterozygosity may be retained when chr loss occurs after WGD. "Complex chromosome rearrangement," "partial chromosome gain and loss," and abbreviations as in Figure 1.

Wilcoxon-Mann–Whitney test). In all WGD gliomas combined, most chr segments showing copy-number losses were heterozygous (74% in ODG; 72% in astrocytomas; 73% in GBM), indicating that at least 3-quarters of chr losses occurred after WGD in tetraploid gliomas (*data not shown*). Among *IDH*m gliomas with WGD, all 4 ODG had 2 homozygous copies of chr 1p and 19q, and 6/7 astrocytomas (initial and recurrent tumors included) had 3 or 4 homozygous copies of chr 17p harboring *TP53* gene. The recurrent absence of heterozygosity suggests that 1p/19q codeletion and 17p CNLOH occurred before WGD.

CT is Less Frequent in *IDHm* Gliomas Compared to GBM and Only Occurs in Grade 3 or 4 Astrocytomas

CT occurred significantly less frequently in *IDH*m gliomas as a whole than in GBM (4.7% versus 18.7%, $P = .0008$, chi-square test). There was a trend towards a lower frequency of CT in grade 3 or 4 *IDH*m astrocytomas compared to GBM (9.2% vs. 18.7%, $P = .0982$, chi-square test). CT was detected in 5 high-grade *IDH*m astrocytomas (4 grade 3, 1 grade 4) at initial diagnosis (5/105 *IDH*m gliomas, 4.7%). No ODG or grade 2 astrocytoma displayed CT patterns. Only one astrocytoma (grade 3) displayed both CT and WGD; the retention of heterozygosity of the chr segments showing copy-number loss indicates WGD occurred prior to CT. CT was detected in 4 recurrent *IDH*m astrocytomas (all grade 4; 4/17 recurrent astrocytomas, 23.5%). The initial tumor was available in only 1 case (with CT on chr 3q), which also displayed WGD solely at recurrence (with retention of heterozygosity indicating that WGD occurred before CT); CT and WGD were both absent from the initial tumor. Chr regions affected by CT in *IDH*m astrocytomas and key gene alterations are presented in Table 1. CT was associated with *CDKN2A/B* HD in 3 grade 4 astrocytomas and with *MYCN* amplification in one grade 3 astrocytoma. One example of CT in *IDH*m astrocytomas is presented in Figure 4C.

Chr regions affected by CT in GBM are presented in Table 2. *CDK4* and *MDM2* amplifications were strongly associated with CT in GBM ($P < .0001$, Fisher's exact test; $P = .0091$, chi-square test, respectively). We did not find an association between CT and *EGFR* amplification ($P = .1004$, chi-square test) or *CDKN2A/B* HD ($P = .8546$, chi-square test). Only 3 GBM displayed both CT and WGD (one of them with retention of heterozygosity indicating the occurrence of WGD before CT).

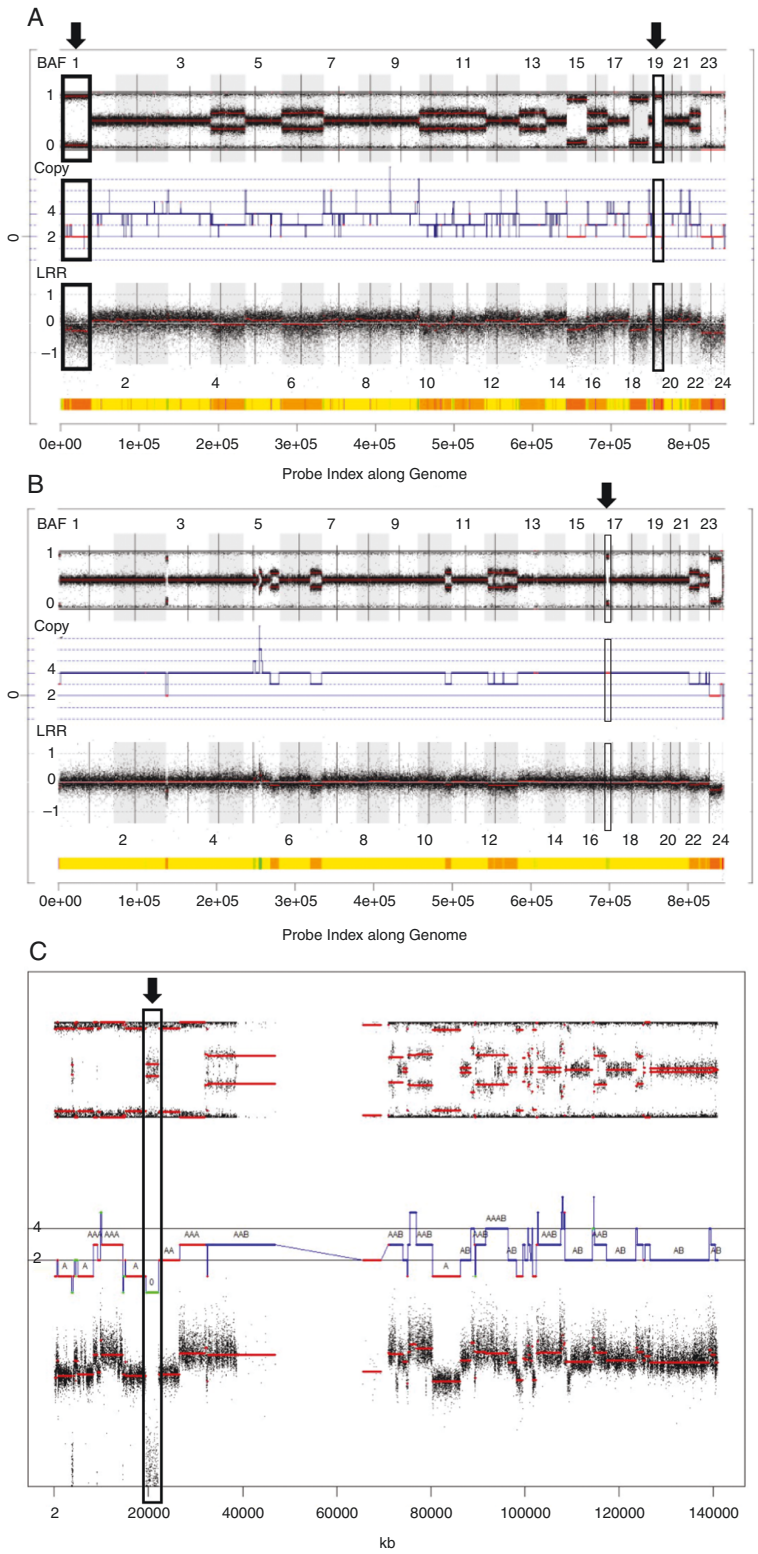

Figure 4. Analysis of *IDH*-mutant gliomas with the *GAP* method and *CTLPScanner*. (A) Genomic profile of a WHO grade 3 ODG with WGD. Frames: 2 copies of homozygous allelotype (red line) of chr 1p and 19q, suggesting occurrence of 1p/19q codeletion prior to WGD. (B) Genomic profile of a WHO grade 4 astrocytoma with WGD. Frames: 4 copies of homozygous allelotype of 17p, suggesting occurrence of CNLOH on 17p prior to WGD. (A-B) Most genomic regions with chr loss (except 1p, 19q, and 17p) displayed 3 copies of heterozygous allelotype, indicating prior occurrence of WGD. (C) Genomic profile of a WHO grade 4 astrocytoma with CT on chr 9. Frames: *CDKN2A/B* HD. Abbreviations as in Figure 1 and HD, homozygous deletion; LOH, loss of heterozygosity.

Table 1. Chromosomal Regions Affected by CT in *IDH*-Mutant Astrocytomas

Chr(s)	Chromosomal region	Size (Mb)	Tumor occurrence (*n*°)	Gene alteration
Tumor at initial diagnosis				
2	2p22.3-p25.3	35	first	*nMYC* Amp
4	4q31.21-q35.2	45	first	
9	9p21.1-24.3 9q21.12-q33.3	30 55	first	*CDKN2A/B* HD
10	10p15.3-q25.3	115	first	
11	11p14.1-p15.5	30	first	
Tumor at recurrence				
3	3q25.2-q29	40	second	
7	7p15.3-p21.3	15	second	
9	9p13.3-p23	25	fourth	*CDKN2A/B* HD
9	9p21.1-p24.1	20	fourth	*CDKN2A/B* HD
			fifth	*CDKN2A/B* HD

CT, chromothripsis; Amp, amplification; HD, homozygous deletion; chr, chromosome(s).

CT and WGD Were Not Associated With Prognosis in the Cohort

OS did not significantly differ in GBM with versus without WGD (14.5 vs. 12.5 months, respectively, $P = .5663$, log-rank test) and in GBM with versus without CT (17 versus 12 months, respectively, $P = .4597$, log-rank test). OS did not significantly differ in *IDHm* gliomas with versus without WGD (98 vs. 196 months, respectively, $P = .7952$, log-rank test) and in *IDHm* gliomas with versus without CT (230 vs. 261 months, respectively, $P = .4068$, log-rank test). However, the subgroups were small and median OS was not reached for grade 2 *IDHm* gliomas. No OGD displayed CT patterns. Kaplan–Meier curves for GBM and *IDHm* gliomas are shown in Figure 5.

Discussion

We studied WGD and CT, both associated with genome instability, in a cohort of 297 adult-type diffuse gliomas. To the best of our knowledge, this is the largest study on CIN in adult-type diffuse gliomas independent from the *TCGA*. The present work shows for the first time that WGD is as frequent in *IDH*m gliomas as in GBM, while still rare (<10%) in diffuse gliomas compared to other types of cancer. WGD was an early event occurring prior to most chr losses (>75%), which facilitates the occurrence of CNV. Key driver CNV occurred in most instances (if not always) before WGD, such as 1p/19q codeletion in ODG and 17p CNLOH/loss in astrocytomas. CT was significantly less frequent in *IDH*m gliomas as a whole compared to GBM ($P = .0008$). It occurred in some high-grade (grade 3 or 4) *IDH*m astrocytomas (9.2%) but was not detected in ODG, whatever the grade, or in grade 2 *IDH*m astrocytomas. We could not show an association between WGD or CT occurrence and OS but median OS was not reached in grade 2 tumors.

In cancer, WGD and CT contribute to genome instability, on the genome-scale for the former and on the chr scale for the latter. Genome instability is a hallmark of cancer: It allows tumor cells to acquire oncogenic properties through key genetic alterations.[26] CIN is a dynamic process giving rise to genome diversity, necessary to select more aggressive subclones, drivers of tumor evolution, and treatment resistance. Two types of CIN were proposed: numerical CIN (gains and losses of whole chr) and structural CIN (eg, rearrangements, amplifications, and HD).[5] WGD would lead to numerical CIN, whereas CT would lead to structural CIN. Those 2 types of genome remodeling are not mutually exclusive. They have been little studied in diffuse gliomas compared to other tumor types.

WGD is a frequent genetic event in many cancers (occurring in around 30% of advanced cancers), providing a survival advantage to tumor cells.[7,27] WGD allows the latter to overcome deleterious gene alterations by buffering DNA losses. One of our previous works showed that WGD occurs in about 10% of GBM, leading to numerous CNV.[9] WGD has not been studied in *IDH*m gliomas before. The present study demonstrates that WGD also results in CNV in *IDH*m gliomas. ODG and grade 3 astrocytomas with WGD displayed an increased CNV load compared to the same tumor types without WGD. Our results concur with those of the *TCGA* which show that tumors with WGD are more prone to aneuploidy (mostly through chr losses) compared to tumors without WGD.[28] Tetraploid cells shed excess DNA to reach an optimal genome equilibrium. WGD is associated with whole chr gains or losses (compared to chr arm-only alterations), arguing for chr missegregation in tumors with WGD.[29] In our study, most chr losses occurred after WGD, suggesting that WGD confers aneuploidy tolerance and propagates CIN. However, in our cohort, 2 key CNV in *IDH*m gliomas (ie, 1p/19q codeletion in ODG and CNLOH/17p loss in astrocytomas) occurred before WGD. This result concurs with that of Jamal-Hanjan et al., who

Table 2. Chromosomal Regions Affected by CT in GBM

Chr(s)	Chromosomal region	Size (Mb)	Number of tumors	Gene alteration
Cases with CT on one chr				
12	12q14.1-q15	15	5	*CDK4* Amp (4/5) *MDM2* Amp (5/5)
	12q13.2-q15	15	1	*CDK4/MDM2* Amp
	12q12-q14.1	20	1	*CDK4* Amp
	12q14.1-q21.1	20	1	*CDK4/MDM2* Amp
	12q24.11-q24.22	10	1	
	12q12-q21.31	45	1	*CDK4/MDM2* Amp
	12q14.3-q15	5	1	*MDM2* Amp
	12p11.21-p12.1 12q13.2-q22	10 40	1	*KRAS* Amp *CDK4/MDM2* Amp
	12p11.21-p12.3	15	1	*KRAS* Amp
9	9p21.1-p21.3	15	3	*CDKN2A/B* HD (3/3)
	9p21.1-p23	20	1	*CDKN2A/B* HD
	9p21.3-p24.1	15	1	*CDKN2A/B* HD
	9p21.2-p22.2	10	1	*CDKN2A/B* HD
	9p13.2-24.3	35	1	*CDKN2A/B* HD
7	7p11.2-p22.3	55	1	*EGFR* Amp
	7p12.1-q21.3	50	1	*EGFR* Amp *MET/CDK6* Amp
	7p11.2-p14.1	20	1	*EGFR* Amp
1	1p32.3-p36.12	30	1	*CDKN2C* HD
	1p36.22-p36.32	5	1	
4	4q12-q34.1	120	1	*PDGFRA* Amp
10	10q11.21-q23.1	40	1	
11	11p11.12-15.5	50	1	
13	13q31.1-q33.3	25	1	
14	14q12-q24.2	50	1	
19	19q13.32-q13.43	15	1	
Cases with CT on 2 chrs				
10 13	10p11.21-p12.1 13q21.31-q32.2	13 35	1	*RB1* HD
1 9	1p35.2-p36.33 9p21.1-p24.3	30 30	1	*CDKN2A/B* HD
7 10	7p12.1-p15.3 10q21.3-25.3	30 55	1	
2 6	2p12-p14 6q12-q27	15 110	1	
6 9	6q25.3-q27 9p21.1-p23	5 20	1	*CDKN2A/B* HD

CT, chromothripsis; GBM, glioblastomas; Amp, amplification; HD, homozygous deletion; chr, chromosome(s).

demonstrated that WGD is an early event, albeit happening after the very first driver events in tumorigenesis.[11] Of note, the sole grade 2 *IDH*m astrocytoma with WGD in our cohort already displayed *TP53* inactivation through CNLOH on 17p. Despite their protracted course (OS may reach 15 to 20 years), ODG harbor aneuploidy from the onset (very early occurrence of 1p/19q codeletion). However, those tumors remained, in our cohort, genomically stable, with few or no additional CNV, especially in grade 2 ODG, in contrast to *IDH*m astrocytomas.

Our work shows that CT is significantly less frequent in *IDH*m gliomas as a whole compared to GBM ($P = .0008$). In the former, CT only occurred in grade 3 or 4 astrocytomas. We could not reliably compare grade 4 *IDH*m astrocytomas and grade 4 *IDH*-wild-type GBM since our cohort only comprised one newly diagnosed grade 4 *IDH*m astrocytoma.

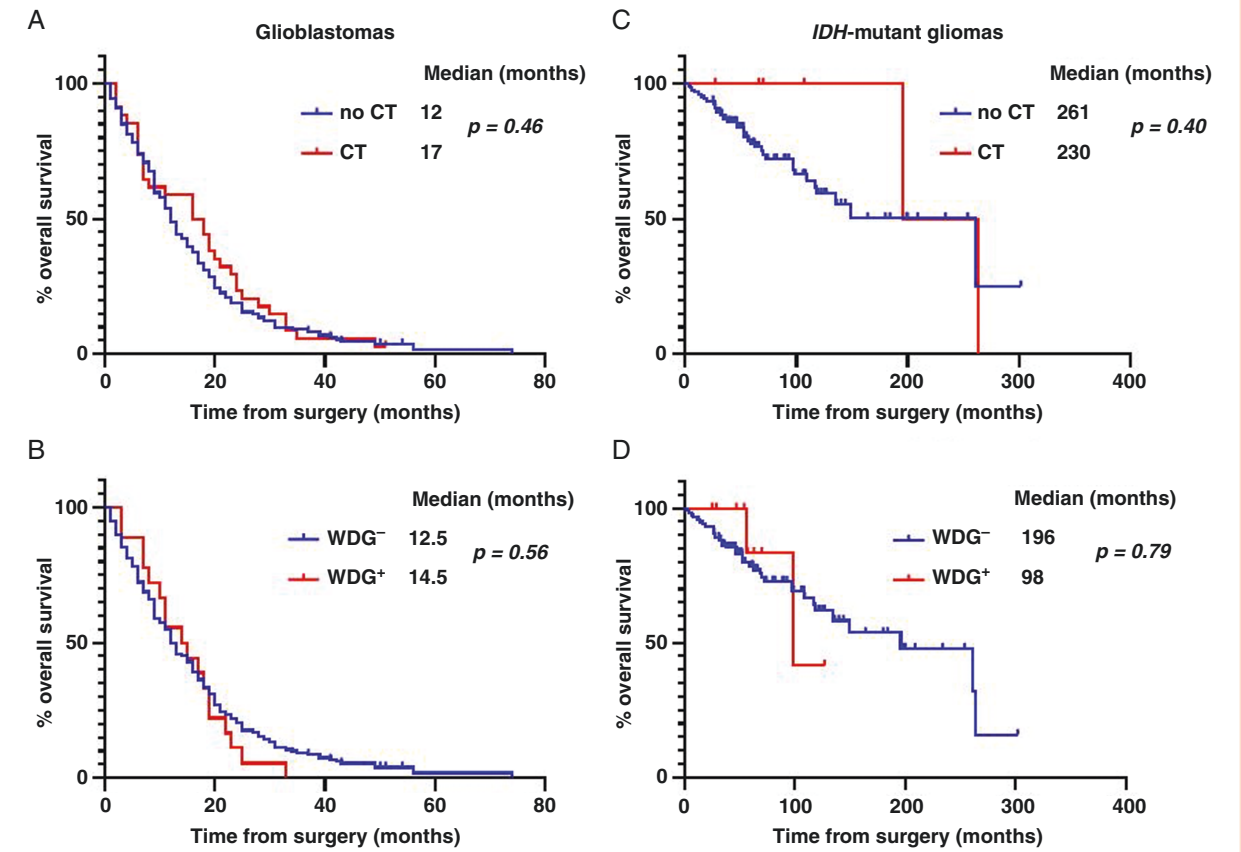

Figure 5. Overall survival in GBM and *IDH*-mutant gliomas with and without CT or WGD. (A) Kaplan–Meier survival curves in GBM according to CT status and (B) to WGD status. (C) Kaplan–Meier survival curves in *IDH*-mutant gliomas according to CT status and (D) to WGD status. There was no statistically significant association between overall survival and CT or WGD in GBM or *IDH*-mutant gliomas. Median overall survival was not reached in grade 2 *IDH*-mutant gliomas. CT, chromothripsis; WGD, whole-genome duplication.

CT may contribute to marked genome remodeling in some high-grade astrocytomas. The present study confirms that CT on 9p may lead to *CDKN2A/B* HD, which is the most important molecular prognostic factor in *IDH*m astrocytomas, warranting WHO grade 4.[30–32] *MYCN* amplification, which has been found to be closely associated with OS, was detected in association with CT in one grade 3 astrocytoma in our cohort.[30] The absence of CT in grade 2 or 3 ODG in our study is in line with the stable genome and prolonged OS observed in those tumors compared to *IDH*m astrocytomas and GBM. The absence of CT in ODG may be explained, in part, by the absence of *TP53* mutation in ODG compared to most *IDH*m astrocytomas and some GBM. *TP53* plays a central role in maintaining genome stability. *TP53* mutation has been linked to CT occurrence in medulloblastoma in Li-Fraumeni patients and in acute myeloid leukemia.[20,33] *TP53* mutation predisposes cells to CT and facilitates cell survival following catastrophic DNA rearrangements. Inversely, *IDH* mutation may protect tumor cells, to some extent, from genome instability, as reflected by the less frequent occurrence of CT in *IDH*m gliomas compared to GBM. *IDH* mutation leads to a hypermethylated phenotype, also known as "CpG island methylator phenotype" (CIMP).[34] Genome hypermethylation may shield DNA from catastrophic genetic events, unlike hypomethylation which favors genome instability.[35]

Interestingly, in a cohort of 94 diffuse gliomas (including 11 cases with CT), Cohen et al. showed that CT was more frequent in grade 4 *IDH*m astrocytomas compared to lower-grade tumors and more frequent in *IDH*m gliomas (all 1p/19q intact) compared to *IDH*-wild-type gliomas (most being GBM according to the 2021 WHO classification).[36] However, the authors could not conclude whether the massive intrachromosomal instability detected occurred as a one-time event ("true" CT) or in sequential events over time (severe CIN).[36] Moreover, DNA was extracted from formalin-fixed paraffin-embedded samples, and not fresh-frozen material (as in our study), which makes detecting fine genomic alterations such as CT difficult. The criteria used for CT diagnosis were not as stringent as ours and the chr regions involved were not mentioned. CT prevalence varies from one study to another depending on the molecular biology techniques and diagnostic criteria used. In this work, we combined manual screening and bioinformatic analyses to assess CT patterns according to previously established, stringent criteria.[24] Of note, previous work on SNP arrays from the *TCGA* found a prevalence of CT in GBM similar to that in our study (16% and 18.7%, respectively).[8]

We could not show an association between CT occurrence and OS in GBM and grade 3 or 4 *IDH*m astrocytomas (OS was not reached in grade 2 astrocytomas). CT has been shown to be a negative prognostic marker in some cancers, such as acute myeloid leukemia, medulloblastoma, melanoma, colorectal cancer, and recently GBM.[22,37–41] Steele et al. identified signatures of CNV in human cancer; one of the signatures enriched in CT events was associated with shorter OS in GBM but the difference was not statistically significant.[37] With regards to *IDH*m gliomas, a study on a larger cohort with a longer follow-up may show worse prognosis in CT cases. Chr shattering will break apart multiple genes and may yield multiple oncogenic alterations in a one-time event. CT events are enriched in known cancer drivers and are associated with gene amplifications, as illustrated by the strong correlation with *MDM2/CDK4* amplifications in our GBM cases ($P < .0001$).[14–16] HD of tumor suppressor genes, such as *CDKN2A/B*, may also occur within CT regions, as observed in our study.[9,22] Last but not least, CT may generate oncogenic gene fusions that may drive tumor development and/or progression and may be treated with targeted therapies.[6,31] The novel, unique gene junctions resulting from chr rearrangements can also promote the production and presentation of neoantigens, which can activate immune cells.[42] Conversely, CT has been linked to immune evasion and resistance to immunotherapy in human carcinomas.[43] The failure of immunotherapeutic approaches to improve survival in GBM might be due in part to the immunologically "cold" microenvironment of those tumors.[44] Interestingly, in CT, inappropriate exposure of nuclear DNA (during chr shattering) to the cytosol activates the cGAS-STING pathway, which induces type I Interferon responses and tumor suppressive effects.[45] This pathway is known to be suppressed in GBM which might, in part, explain the poor response rates to immunotherapy. Activating sensing of DNA damage and the cGAS/STING pathway may sensitize CT-rearranged GBM to immunotherapy. Of note, high tumor aneuploidy has been shown to correlate with immune evasion and reduced response to immunotherapy in 12 human cancer types.[46] Detecting CT, and more broadly aneuploidy, may help identify patients most likely to respond to immunotherapy.

In our series, there was no association between the occurrence of CT and WGD in GBM. However, such an association has been shown in Cortés-Ciriano et al.'s study with WGD occurring prior to CT (and favoring CT occurrence) among 38 cancer types.[19] WGD is rare in *IDH*m gliomas and GBM (<10%) compared to carcinomas. Once again, a larger cohort may allow us to show an association between WGD and CT and between CT and shorter OS.

Finally, our work validates that the number of CNV increases with the histological grade of *IDH*m gliomas, underlining that high-grade tumors are more genomically unstable than lower-grade tumors.[47] Recently, large aneuploidy changes have been found to portend a poor prognosis in grade 2 or 3 *IDH*m astrocytomas.[48] The CNV load was already increased in those tumors with short OS, whereas the mutation burden (point mutations per megabase) was not significantly different.[49] This suggests that CIN, rather than the mutation load, is the critical factor in the progression to more aggressive tumors.[49] In *IDH*m astrocytomas, a higher CNV burden was associated with *CDKN2A/B* HD and CT occurrence.[50] As previously mentioned, most *IDH*m astrocytomas display *TP53* mutation, a risk factor for aneuploidy and CT.[49] Detecting CIN in grade 2 astrocytomas suggests it occurs before tumor progression, and most likely contributes to it. Assessing genome instability early in the disease may help better evaluate prognosis and adapt treatments. In the present study, ODG displayed no or few CNV superimposed on the early 1p/19q codeletion.

As for the limits of the study, the retrospective nature of the series may be a selection bias, although all interpretable SNP array cases involving fresh-frozen tumor tissue were included in this work. The prolonged survival of *IDH*m gliomas hindered, in part, the survival analysis (OS not reached in grade 2 tumors). SNP array data provide a lower resolution than whole-genome sequencing for detecting CT and only allows to evaluate some criteria of Korbel and Campbell.[24] However, a combined approach with manual screening and bioinformatic analysis improves the reliability of CT detection.

In summary, CT was significantly less frequent in *IDH*m gliomas as a whole compared to GBM. It was not detected in ODG, whatever the grade, or in grade 2 *IDH*m astrocytomas. Leading to genome remodeling, CT might fuel tumor progression and aggressive behavior in adult diffuse gliomas. WGD arises as often in GBM as in *IDH*m gliomas, of any type or grade. In both tumor types, WGD is a rare and early event that contributes to aneuploidy. Although preventing or treating defects in chr segregation is beyond the reach of medicine so far, detecting CIN at an early stage of the disease may help anticipate tumor progression and provide the most suitable care (eg more aggressive treatments in low-grade *IDH*m gliomas, even after complete resection). Prospective studies on larger cohorts with longer follow-ups are needed to evaluate the prognostic impact of WGD and CT in glioma patients.

Supplementary material

Supplementary material is available online at *Neuro-Oncology* (https://academic.oup.com/neuro-oncology).

Keywords

chromothripsis | genome instability | glioblastoma | *IDH*-mutant glioma | whole-genome duplication

Funding

None declared.

Acknowledgments

The authors thank Prof Patrick Saulnier (INSERM U1066, CNRS 6021, Angers University Hospital) for his advice on statistical analyses.

Conflict of interest statement

The authors declare no conflicts of interest.

Authorship statement

Data analysis (B.S., L.B., A.F.); Writing (B.S., L.B., A.F., A.R.); Technical support (L.B.); Editing (B.S., A.F., E.G., A.R.); Study design (A.R.).

Data availability

SNP array data in this study are available in the public repository ArrayExpress under the accession number E-MTAB-13542, under the following link:
https://www.ebi.ac.uk/biostudies/arrayexpress/studies/E-MTAB-13542?key=edfc705d-9286-4683-bb46-7366692896aa

Affiliations

Department of Pathology, University Hospital of Angers, Angers, France (B.S., L.B., A.F., A.R.); Univ Angers, Nantes Université, Inserm, CNRS, CRCI2NA, SFR ICAT, F-49000 Angers, France (B.S., L.B., A.F., E.G., A.R.)

References

1. Louis DN, eds. *The 2021 WHO Classification of Tumours of the Central Nervous System*. Lyon: International Agency for Research on Cancer, 2021.
2. Jenkins RB, Blair H, Ballman KV, et al. A t(1;19)(q10;p10) mediates the combined deletions of 1p and 19q and predicts a better prognosis of patients with oligodendroglioma. *Cancer Res*. 2006;66(20):9852–9861.
3. Yan H, Parsons DW, Jin G, et al. IDH1 and IDH2 mutations in gliomas. *N Engl J Med*. 2009;360(8):765–773.
4. Stupp R, Mason WP, van den Bent MJ, et al; European Organisation for Research and Treatment of Cancer Brain Tumor and Radiotherapy Groups. Radiotherapy plus concomitant and adjuvant temozolomide for glioblastoma. *N Engl J Med*. 2005;352(10):987–996.
5. Vishwakarma R, McManus KJ. Chromosome instability; implications in cancer development, progression, and clinical outcomes. *Cancers (Basel)*. 2020;12(4):824.
6. Baker TM, Waise S, Tarabichi M, Van Loo P. Aneuploidy and complex genomic rearrangements in cancer evolution. *Nat Cancer*. 2024;5(2):228–239.
7. Bielski CM, Zehir A, Penson AV, et al. Genome doubling shapes the evolution and prognosis of advanced cancers. *Nat Genet*. 2018;50(8):1189–1195.
8. Zack TI, Schumacher SE, Carter SL, et al. Pan-cancer patterns of somatic copy number alteration. *Nat Genet*. 2013;45(10):1134–1140.
9. Boisselier B, Dugay F, Belaud-Rotureau MA, et al. Whole genome duplication is an early event leading to aneuploidy in IDH-wild type glioblastoma. *Oncotarget*. 2018;9(89):36017–36028.
10. Ganem NJ, Storchova Z, Pellman D. Tetraploidy, aneuploidy and cancer. *Curr Opin Genet Dev*. 2007;17(2):157–162.
11. Jamal-Hanjani M, Wilson GA, McGranahan N, et al; TRACERx Consortium. Tracking the evolution of non-small-cell lung cancer. *N Engl J Med*. 2017;376(22):2109–2121.
12. Dewhurst SM, McGranahan N, Burrell RA, et al. Tolerance of whole-genome doubling propagates chromosomal instability and accelerates cancer genome evolution. *Cancer Discov*. 2014;4(2):175–185.
13. Stephens PJ, Greenman CD, Fu B, et al. Massive genomic rearrangement acquired in a single catastrophic event during cancer development. *Cell*. 2011;144(1):27–40.
14. Luijten MNH, Lee JXT, Crasta KC. Mutational game changer: Chromothripsis and its emerging relevance to cancer. *Mutat Res Rev Mutat Res*. 2018;777:29–51.
15. Ostapińska K, Styka B, Lejman M. Insight into the molecular basis underlying chromothripsis. *Int J Mol Sci* . 2022;23(6):3318.
16. Shoshani O, Brunner SF, Yaeger R, et al. Chromothripsis drives the evolution of gene amplification in cancer. *Nature*. 2021;591(7848):137–141.
17. Pellestor FC. cataclysms behind complex chromosomal rearrangements. *Mol Cytogenet*. 2019;12(6).
18. Zhang CZ, Leibowitz ML, Pellman D. Chromothripsis and beyond: Rapid genome evolution from complex chromosomal rearrangements. *Genes Dev*. 2013;27(23):2513–2530.
19. Cortés-Ciriano I, Lee JJ, Xi R, et al; PCAWG Structural Variation Working Group. Comprehensive analysis of chromothripsis in 2,658 human cancers using whole-genome sequencing. *Nat Genet*. 2020;52(3):331–341.
20. Rausch T, Jones DT, Zapatka M, et al. Genome sequencing of pediatric medulloblastoma links catastrophic DNA rearrangements with TP53 mutations. *Cell*. 2012;148(1-2):59–71.
21. Torre M, Alexandrescu S, Dubuc AM, et al. Characterization of molecular signatures of supratentorial ependymomas. *Mod Pathol*. 2020;33(1):47–56.
22. Furgason JM, Koncar RF, Michelhaugh SK, et al. Whole genome sequence analysis links chromothripsis to EGFR, MDM2, MDM4, and CDK4 amplification in glioblastoma. *Oncoscience*. 2015;2(7):618–628.
23. Popova T, Manié E, Stoppa-Lyonnet D, et al. Genome Alteration Print (GAP): a tool to visualize and mine complex cancer genomic profiles obtained by SNP arrays. *Genome Biol*. 2009;10(11):R128.
24. Korbel JO, Campbell PJ. Criteria for inference of chromothripsis in cancer genomes. *Cell*. 2013;152(6):1226–1236.
25. Yang J, Liu J, Ouyang L, et al. CTLPScanner: A web server for chromothripsis-like pattern detection. *Nucleic Acids Res*. 2016;44(W1) :W252–W258.
26. Hanahan D, Weinberg RA. Hallmarks of cancer: The next generation. *Cell*. 2011;144(5):646–674.
27. López S, Lim EL, Horswell S, et al; TRACERx Consortium. Interplay between whole-genome doubling and the accumulation of deleterious alterations in cancer evolution. *Nat Genet*. 2020;52(3):283–293.
28. Prasad K, Bloomfield M, Levi H, et al. Whole-genome duplication shapes the aneuploidy landscape of human cancers. *Cancer Res*. 2022;82(9):1736–1752.
29. Mazzagatti A, Engel JL, Ly P. Boveri and beyond: Chromothripsis and genomic instability from mitotic errors. *Mol Cell*. 2024;84(1):55–69.
30. Shirahata M, Ono T, Stichel D, et al. Novel, improved grading system(s) for IDH-mutant astrocytic gliomas. *Acta Neuropathol*. 2018;136(1):153–166.
31. Appay R, Dehais C, Maurage CA, et al; POLA Network. CDKN2A homozygous deletion is a strong adverse prognosis factor in diffuse malignant IDH-mutant gliomas. *Neuro Oncol*. 2019;21(12):1519–1528.

32. Lu VM, O'Connor KP, Shah AH, et al. The prognostic significance of CDKN2A homozygous deletion in IDH-mutant lower-grade glioma and glioblastoma: A systematic review of the contemporary literature. *J Neurooncol*. 2020;148(2):221–229.
33. Rücker FG, Dolnik A, Blätte TJ, et al. Chromothripsis is linked to TP53 alteration, cell cycle impairment, and dismal outcome in acute myeloid leukemia with complex karyotype. *Haematologica*. 2018;103(1):e17–e20.
34. Noushmehr H, Weisenberger DJ, Diefes K, et al; Cancer Genome Atlas Research Network. Identification of a CpG island methylator phenotype that defines a distinct subgroup of glioma. *Cancer Cell*. 2010;17(5):510–522.
35. Pfeifer GP. Defining driver dna methylation changes in human cancer. *Int J Mol Sci* . 2018;19(4):1166.
36. Cohen A, Sato M, Aldape K, et al. DNA copy number analysis of Grade II-III and Grade IV gliomas reveals differences in molecular ontogeny including chromothripsis associated with IDH mutation status. *Acta Neuropathol Commun*. 2015;3(34).
37. Steele CD, Abbasi A, Islam SMA, et al. Signatures of copy number alterations in human cancer. *Nature*. 2022;606(7916):984–991.
38. Voronina N, Wong JKL, Hübschmann D, et al. The landscape of chromothripsis across adult cancer types. *Nat Commun*. 2020;11(1):2320.
39. Fontana MC, Marconi G, Feenstra JDM, et al. Chromothripsis in acute myeloid leukemia: Biological features and impact on survival. *Leukemia*. 2018;32(7):1609–1620.
40. Hirsch D, Kemmerling R, Davis S, et al. Chromothripsis and focal copy number alterations determine poor outcome in malignant melanoma. *Cancer Res*. 2013;73(5):1454–1460.
41. Skuja E, Kalniete D, Nakazawa-Miklasevica M, et al. Chromothripsis and progression-free survival in metastatic colorectal cancer. *Mol Clin Oncol*. 2017;6(2):182–186.
42. Mansfield AS, Peikert T, Smadbeck JB, et al. Neoantigenic potential of complex chromosomal rearrangements in mesothelioma. *J Thorac Oncol*. 2019;14(2):276–287.
43. Zhang Q, Yang L, Xiao H, et al. Pan-cancer analysis of chromothripsis-related gene expression patterns indicates an association with tumor immune and therapeutic agent responses. *Front Oncol*. 2023;13:1074955.
44. Habashy KJ, Mansour R, Moussalem C, Sawaya R, Massaad MJ. Challenges in glioblastoma immunotherapy: Mechanisms of resistance and therapeutic approaches to overcome them. *Br J Cancer*. 2022;127(6):976–987.
45. Low JT, Brown MC, Reitman ZJ, et al. Understanding and therapeutically exploiting cGAS/STING signaling in glioblastoma. *J Clin Invest*. 2024;134(2):e163452.
46. Davoli T, Uno H, Wooten EC, Elledge SJ. Tumor aneuploidy correlates with markers of immune evasion and with reduced response to immunotherapy. *Science*. 2017;355(6322):eaaf8399.
47. Liu Y, Sathe AA, Abdullah KG, et al. Global DNA methylation profiling reveals chromosomal instability in IDH-mutant astrocytomas. *Acta Neuropathol Commun*. 2022;10(1):32.
48. Zhang J, Feng Y, Li G, et al. Distinct aneuploid evolution of astrocytoma and glioblastoma during recurrence. *npj Precis Oncol*. 2023;7(1):97.
49. Richardson TE, Sathe AA, Kanchwala M, et al. Genetic and epigenetic features of rapidly progressing IDH-Mutant astrocytomas. *J Neuropathol Exp Neurol*. 2018;77(7):542–548.
50. Mirchia K, Sathe AA, Walker JM, et al. Total copy number variation as a prognostic factor in adult astrocytoma subtypes. *Acta Neuropathol Commun*. 2019;7(1):92.